

High nuclearity cerium–manganese clusters and their structural and magnetic properties: $\text{Ce}_3^{\text{IV}}\text{Mn}_7^{\text{III}}$ and $\text{Ce}_5^{\text{IV}}\text{Mn}_{11}^{\text{III}}$



Annaliese E. Thuijs, Andrea Marton, Theocharis C. Stamatatos¹, Khalil A. Abboud, George Christou^{*}

Department of Chemistry, University of Florida, Gainesville, FL 32611-7200, USA

ARTICLE INFO

Article history:

Received 29 January 2015

Accepted 19 March 2015

Available online 27 March 2015

Dedicated to Catherine E. Housecroft on the occasion of her 60th birthday.

Keywords:

Manganese

Lanthanide

Single-molecule magnet

Crystal structures

Cerium

ABSTRACT

The syntheses, structures, and magnetic properties are reported of two new high nuclearity Ce–Mn oxo carboxylate clusters at high $\text{Ce}^{\text{IV}}/\text{Mn}^{\text{III}}$ oxidation states and with nuclearities of $\text{Ce}_5\text{Mn}_{11}$ and Ce_3Mn_7 . The compounds are $(\text{N}^{\text{t}}\text{Bu}_4)_2[\text{Ce}_5\text{Mn}_{11}\text{O}_{13}(\text{OH})_2(\text{O}_2\text{CPh})_{24}(\text{NO}_3)_2](\text{NO}_3)$ (**1**) and $[\text{Ce}_3\text{Mn}_7\text{O}_8(\text{O}_2\text{CPh})_{17}(\text{H}_2\text{O})_4]$ (**2**). **1** was prepared from the oxidation of $\text{Mn}(\text{O}_2\text{CPh})_2$ by $(\text{N}^{\text{t}}\text{Bu}_4)_2\text{Ce}(\text{NO}_3)_6$, whereas **2** was obtained from the comproportionation reaction of $\text{Mn}(\text{O}_2\text{CPh})_2$ and $\text{N}^{\text{t}}\text{Bu}_4\text{MnO}_4$ in the presence of $\text{Ce}(\text{NO}_3)_3$. Both compounds possess unprecedented structures, comprising an irregular metal topology of several edge-fused triangular units with overall virtual C_2 symmetry. Variable-temperature, solid-state dc and ac magnetization studies on **1** and **2** in the 1.8–300 K range revealed predominantly weak antiferromagnetic exchange interactions within the complexes. For **1**, the combined dc and ac data indicate an $S = 5$ ground state but with low-lying excited states consistent with the high nuclearity. For **2**, even lower-lying excited states were observed, precluding clear determination of the ground state but with an estimate of $S = 2$ or 3, or less. Complexes **1** and **2** are new additions to the Ce–Mn family of clusters and the broader class of 3d/4f molecular systems, and **1** is the highest nuclearity Ce–Mn cluster to date.

© 2015 Elsevier Ltd. All rights reserved.

1. Introduction

We are continuing in our group to explore polynuclear complexes containing high oxidation state metals such as Ce^{IV} and $\text{Mn}^{\text{III/IV}}$ because of their relevance to a number of areas and applications. The latter include inorganic, organic, biological, environmental, and industrial chemistry for a wide variety of reasons ranging from the often unusual magnetic properties of homo- and heterometallic clusters of Mn through their versatility in oxidizing both inorganic and organic substrates [1–4]. For example, the latter property parallels the catalytic activity of bulk $\text{Ce}^{\text{IV}}/\text{Mn}^{\text{IV}}$ composite oxides previously explored in many applications in sub- and supercritical catalytic wet oxidations for the treatment of wastewater containing toxic organic pollutants such as ammonia, acetic acid, pyridine, phenol, polyethylene glycol, and others [3–6]. Similarly, molecular species such as Ce^{IV} compounds have been employed in homo- and heterogeneous catalysis with Ru complexes for oxidation of water to molecular dioxygen [2], and $\text{Mn}^{\text{III–VII}}$ and Ce^{IV} are commonly employed as oxidants in organic and inorganic synthesis [3,4].

In the molecular magnetism field, the synthesis of Mn^{III} containing clusters continues to be an important source of new single-molecule magnets (SMMs), which are individual molecules capable of functioning as nanoscale magnetic particles and thus represent a bottom-up molecular approach to nanomagnetism [7,8]. Molecular clusters of Mn containing at least some Mn^{III} display a common propensity to possess high ground state spin (S) values, and when coupled with the significant easy-axis-type magnetoanisotropy (negative zero-field splitting parameter, D) resulting from Mn^{III} Jahn–Teller axial elongations, they may also be SMMs [9]. In addition, they can also display other fascinating properties such as quantum tunneling of magnetization (QTM) [10] and quantum phase interference [11].

The inclusion of lanthanide ions into Mn^{III} clusters has also become strongly prevalent in the field during the last decade due to the additional anisotropy provided by the orbital angular momentum of many lanthanides [12–15]. Ce holds a special place among the lanthanides due to its ability to exist in two stable oxidation states, III and IV, under normal conditions. Within the field of SMMs, Ce^{III} is of much greater interest than Ce^{IV} due to the anisotropy Ce^{III} can contribute in addition to the spin of $S = 1/2$, whereas Ce^{IV} is diamagnetic [16]. However, the two oxidation states of Ce can also give rise to interesting electrochemical properties, especially when coupled to 3d metal ions bearing multiple oxidation states, such as Mn [4,6]. Additionally, the oxophilic

^{*} Corresponding author. Fax: +1 352 392 8757.

E-mail address: christou@chem.ufl.edu (G. Christou).

¹ Present address: Department of Chemistry, Brock University, St. Catharines, Ontario L2S 3A1, Canada.

nature of Ce^{III} and Ce^{IV} fosters the formation of hard O²⁻ ions, which when combined with Mn ions yields a promising route to high nuclearity oxide-bridged mixed-metal clusters [17]. Herein we report two new Ce^{IV}–Mn^{III} clusters at high oxidation states and possessing uncommonly large metal nuclearities and unprecedented structures. These clusters were obtained using Mn carboxylate and Ce nitrate sources in MeNO₂ and include the highest nuclearity cluster yet observed in Ce–Mn chemistry, Mn₁₁Ce^{IV}, as well as a new Mn^{III}Ce^{IV}.

2. Experimental

2.1. Syntheses

All manipulations were performed under aerobic conditions using materials and solvents as received. NⁿBu₄MnO₄, (NⁿBu₄)₂Ce(NO₃)₆, and Mn(O₂CPh)₂·4H₂O complexes were prepared using the procedures reported previously [18,19].

2.1.1. (NⁿBu₄)₂[Ce^{IV}Mn^{III}O₁₃(OH)₂(O₂CPh)₂₄(NO₃)₂](NO₃) (1)

To a hot stirred solution of benzoic acid (1.00 g, 8.25 mmol) in nitromethane (20 mL) was added solid Mn(O₂CPh)₂ (0.75 g, 2.25 mmol). The reaction was stirred for 5 min after which solid (NⁿBu₄)₂Ce(NO₃)₆ (1.01 g, 1.00 mmol) was added in small portions. The solution was stirred for a further 10 min and filtered hot. The filtrate was left to concentrate for a period of 5 days, during which small dark brown block-like crystals of 1.7MeNO₂ formed. For the X-ray crystallographic studies, crystals were maintained in mother liquor to prevent degradation until a suitable crystal was selected. Otherwise, the crystals were collected by filtration, washed with hexanes, and dried under vacuum; the yield was 40% based on Mn. *Anal. Calc.* (Found) for 1.5MeNO₂ (C₂₀₅H₂₀₉Ce₅Mn₁₁N₁₀O₈₂): C, 45.35 (45.57); H, 3.88 (3.90); N, 2.58 (2.67)%. Selected IR data (KBr, cm⁻¹): 3422 (w), 3060 (m), 3027 (w), 2533 (w), 1963 (w), 1914 (w), 1819 (m), 1690 (s), 1605 (vs), 1569 (vs), 1493 (s), 1420 (vsb), 1384 (s), 1176 (s), 1155 (m), 1068 (m), 1025 (m), 1002 (w), 936 (w), 839 (m), 814 (m), 720 (s), 686 (sb), 607 (mb), 530 (m), 464 (w), 419 (w).

2.1.2. [Ce^{IV}Mn^{III}O₈(O₂CPh)₁₇(H₂O)₄] (2)

To a hot stirred solution of benzoic acid (1.00 g, 8.25 mmol) in nitromethane (20 mL) was added solid Mn(O₂CPh)₂ (0.75 g, 2.25 mmol). The solution was stirred for five minutes before solid Ce(NO₃)₃ (0.87 g, 2.00 mmol) was slowly added causing a color change from pale pink to deep red. To this solution was added solid NEt₄Br (0.10 g, 0.50 mmol), the solution stirred for a further 5 min, and then solid NⁿBu₄MnO₄ (0.18 g, 0.50 mmol) was added slowly in small portions over 2 min. The reaction was stirred for a further 10 min and filtered hot. The filtrate was allowed to slowly concentrate over 5 days during which time reddish brown block-like crystals of 2.6MeNO₂ formed. For the X-ray crystallographic studies, crystals were maintained in mother liquor to prevent degradation until a suitable crystal was selected. Otherwise, the crystals were collected by filtration, washed with hexanes and dried under vacuum; the yield was 30% based on Mn. *Anal. Calc.* (Found) for 2.2MeNO₂ (C₁₂₁H₉₉Ce₃Mn₇N₂O₅₀): C, 45.62 (45.65); H, 3.21 (3.13); N, 0.88 (0.75)%. Selected IR data (KBr, cm⁻¹): 3413 (mb), 3063 (m), 1596 (s), 1543 (s), 1493 (m), 1414 (vs), 1177 (m), 1069 (m), 1025 (m), 1000 (w), 938 (w), 845 (m), 821 (w), 718 (s), 683 (m), 658 (m), 615 (m), 583 (m), 434 (m).

2.2. General and physical measurements

Elemental analyses (C, H and N) were performed by the in-house facilities of the University of Florida Chemistry

Department. Infrared spectra in the 400–4000 cm⁻¹ range were recorded in the solid state (KBr pellets) on a Nicolet Nexus 670 FTIR spectrometer. Variable temperature dc and ac magnetic susceptibility data down to 1.8 K were collected using a Quantum Design MPMS-XL SQUID magnetometer equipped with a 7 T dc magnet. Magnetization versus field and temperature data were fit using the program MAGNET [20]. Pascal's constants were used to estimate the diamagnetic corrections, which were subtracted from the experimental susceptibilities to give the molar magnetic susceptibilities (χ_M) [21]. Microcrystalline samples were restrained in eicosane to avoid torquing.

2.3. X-ray crystallography

Data were collected at 173 K on a Siemens SMART PLATFORM equipped with a CCD area detector and a graphite monochromator utilizing Mo Kα radiation (λ = 0.71073 Å). Cell parameters were refined using up to 8192 reflections. A full sphere of data (1850 frames) was collected using the ω-scan method (0.3° frame width). The first 50 frames were re-measured at the end of data collection to monitor instrument and crystal stability (maximum correction on I was <1%). Absorption corrections by integration were applied based on measured indexed crystal faces. The structures were solved by the direct methods in SHELXTL6 [22] and refined using full-matrix least-squares cycles. The non-hydrogen atoms were refined anisotropically, whereas the hydrogen atoms were placed in idealized, calculated positions and refined isotropically as riding on their respective carbon atoms.

For 1.7MeNO₂, the asymmetric unit consists of the cluster anion, two NⁿBu₄⁺ cations, one nitrate anion, and seven nitromethane solvent molecules of crystallization. The solvent molecules and the nitrate anion were disordered and could not be modeled properly, thus program SQUEEZE [23], a part of the PLATON package of crystallographic software, was used to calculate the solvent disorder area and remove its contribution to the overall intensity data. Distances and angles of the counter ions were constrained to maintain ideal values during the refinement. Three benzoate ligands were disordered and were resolved: Ligand C310 was refined in two parts while ligands C340 and C370 were refined in three parts each. A total of 2232 parameters were included in the final cycle of refinement using 29762 reflections with I > 2σ(I) to yield R₁ and wR₂ of 6.96 and 17.99%, respectively.

For complex 2.6MeNO₂, the asymmetric unit consists of the Ce₃Mn₇ cluster and six nitromethane solvent molecules. The latter were disordered and could not be modeled properly, thus program SQUEEZE was again used to calculate the solvent disorder area and remove its contribution to the overall intensity data. The eight coordinated water protons were obtained from a difference Fourier map and were refined as riding on their parent oxygen atoms. A total of 1576 parameters were included in the final cycle of refinement using 13934 reflections with I > 2σ(I) to yield R₁ and wR₂ of 7.35 and 14.38%, respectively.

Unit cell data and the final refinement indices R₁ and wR₂ are listed in Table 1.

3. Results and discussion

3.1. Syntheses

Most of the known Mn/Ce clusters to date have been synthesized under ambient conditions by the oxidation of a Mn^{II} salt by a Ce^{IV} source, often in the presence of a carboxylate source and in the presence or absence of chelating ligands. Such procedures have successfully led to the preparation of a number of heterometallic Ce/Mn products [24]. Some of the more notable of

Table 1
Crystal data and structure refinement parameters for complexes **1** and **2**.

	1·7MeNO ₂	2·6MeNO ₂
Formula ^a	C ₂₀₈ H ₂₁₆ Ce ₅ Mn ₁₁ N ₁₂ O ₈₅	C ₁₂₅ H ₁₁₁ Ce ₃ Mn ₇ N ₆ O ₅₈
Fw (g mol ⁻¹)	5548.87	3430.14
Space group	P1	P2 ₁ /n
a (Å)	20.3396(14)	28.964(3)
b (Å)	20.7771(14)	17.1760(17)
c (Å)	31.128(2)	29.677(3)
α (°)	96.975(1)	90
β (°)	103.792(1)	114.339(2)
γ (°)	115.530(1)	90
V (Å ³)	11150.5(13)	13451(2)
Z	2	4
T (K)	173(2)	100(2)
Radiation (Å) ^b	0.71073	0.71073
ρ _{calc} (g cm ⁻³)	1.653	1.694
μ (mm ⁻¹)	1.690	1.723
R ₁ ^{c,d}	0.0696	0.0735
wR ₂ ^e	0.1799	0.1438

^a Including solvent molecules.

^b Graphite monochromator.

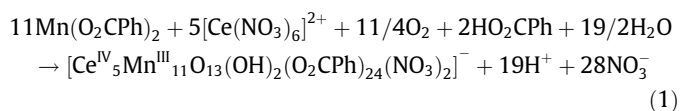
^c I > 2σ(I).

^d R₁ = 100Σ(|F_o - |F_c||)/Σ|F_o|.

^e wR₂ = 100[Σ[w(F_o² - F_c²)²]/Σ[w(F_o²)²]]^{1/2}, w = 1/[Σ²(F_o²) + [(ap)² + bp], where p = [max(F_o², 0) + 2F_o²]/3.

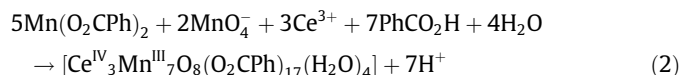
these include the several Ce^{IV}_xMn^{IV}_y aggregates that were the first Ce/Mn molecular clusters to be reported [24], as well as family of Ce^{IV}Mn^{III}₈ complexes, and Ce₂Ce₂Mn^{III}₁₀, Ce₆Mn^{III}₈, Mn₄Ce₂^{III}, and Mn₂Mn^{III}₂Ce₆^{IV} clusters [17,25–29]. To date, the highest nuclearity in such a molecular cluster has been a Ce₆Mn₈ species [27].

In the present work, we have followed a somewhat similar approach to previous work but with some distinct differences, such as the use of heated rather than room temperature reaction solutions to ensure adequate solubility of all reagents in the MeNO₂ solvent. Other than this, the synthesis of **1** involved the reaction of (NⁿBu₄)₂Ce(NO₃)₆ and Mn(O₂CPh)₂ in a 1:2.25 ratio in MeNO₂ in the presence of an excess of PhCO₂H, yielding a dark brown solution from which was isolated [Mn^{III}₁₁Ce^{IV}₅O₁₃(OH)₂(O₂CPh)₂₄(NO₃)₂] (**1**) in 40% yield. It thus employed a typical Ce^{IV}/Mn^{II} redox reaction in a 1:2.25 ratio, giving a product with essentially the same ratio, i.e. Ce₅Mn₁₁. This is almost certainly coincidental, since in our experience the mixed metal reagent ratio rarely is the same as the ratio in the product from such complicated high nuclearity cluster syntheses. What is more noteworthy, however, is that the Ce^{IV}:Mn^{II} = 1:2.25 ratio is expected to give a Ce^{III}Mn^{III}₁₁ reaction mixture, whereas isolated **1** is Ce^{IV}Mn^{III}_{2.25}, so either there are Mn^{II}-rich products in the filtrate or atmospheric O₂ has provided additional oxidizing equivalents. The fact that the filtrate is still darkly colored, consistent with Mn^{III}, and that **1** contains Ce^{IV}Mn^{III}₁₁ (i.e. not just all-Mn^{III} but also Ce^{IV} not Ce^{III}) suggests the involvement of O₂; thus, Eq. (1) summarizes the proposed redox chemistry involved in the formation of **1**.



This conclusion is in fact consistent with our previous observations of Ce/Mn reaction products at much higher oxidation levels than the metal reagent ratios would predict, which we have rationalized as being due to the greater ease of oxidation of Ce^{III} when within a hard oxide environment, and thus its oxidation by O₂ [29]. In effect the Ce would be acting as a catalyst for the oxidation of Mn^{II} to Mn^{III} by O₂, and such catalytic activity by Ce has indeed already been proposed in the oxidation of alcohols by O₂ catalyzed by a CeMn₆ cluster [30].

The synthesis of **2** employed a new type of reaction in this area, a comproportionation between Mn^{II} and Mn^{VII} in the presence of Ce^{III}. Thus, the reaction in MeNO₂ of Ce(NO₃)₃, Mn(O₂CPh)₂, and NⁿBu₄MnO₄ in a 2:2.25:0.5 ratio in the presence of NEt₄Br and PhCO₂H gave a dark red solution from which was isolated [Ce^{IV}Mn^{III}₇O₈(O₂CPh)₁₇(H₂O)₄] (**2**) in 30% yield. The Mn^{II}:Mn^{VII} ratio gives an ~Mn^{III} average and the total Ce:Mn = 2:2.75, so it is not necessary to invoke the involvement of O₂ to yield **2** in this more complicated stoichiometry, as summarized by Eq. (2).



Additional reactions were, of course, explored with slightly altered Ce:Mn^{II}:Mn^{VII} ratios to attempt to improve the yield of **2**, but they all gave **2** in lower yield and/or mixtures of products. At room temperature, the synthetic procedure to **2** gave instead the previously reported [CeMn₈O₈(O₂CPh)₁₂(L₄)] (L = H₂O or MeNO₂) [25].

3.2. Description of structures

The structure and a stereoview of the [Ce^{IV}Mn^{III}₁₁O₁₃(OH)₂(O₂CPh)₂₄(NO₃)₂]⁻ anion of **1** are shown in Fig. 1. Its [Ce₅Mn₁₁O₁₃(OH)₂]⁴⁺ core contains five Ce^{IV} and eleven Mn^{III} atoms held together by five μ₄-O²⁻, eight μ₃-O²⁻ and two μ₃-OH⁻ ions. The oxidation state of the metal atoms and the protonation levels of the O atoms were determined by inspection of metric parameters, charge considerations, and bond valence sum (BVS) calculations (Tables 2 and 3). Selected interatomic distances and bond angles are available in Table S1. The core contains a [Ce₅O₇(OH)₂] subunit, with the μ₃-OH⁻ ions (O6 and O15) both bridging the central Ce₃ triangle (Ce1, Ce2, Ce3), and this is linked via bridging O²⁻ ions to nine Mn^{III} atoms on one side and two Mn^{III} atoms on the other. Alternatively, the core can be described as an irregular collection of edge-fused metal triangles, tetrahedra and butterfly subunits, all held together by bridging O²⁻ and OH⁻ ions. Peripheral ligation around the core is provided by six μ₃- and eighteen μ-benzoate groups: two of the former (O52/O53 and O56/O57) each bridge a Mn₂Ce unit in the rare η²:η²:μ₃ mode, and the other four bridge Mn₃ units in the η²:η¹:μ₃ mode. The eighteen μ₂-benzoate groups bridge Mn₂ or CeMn pairs in their common *syn*, *syn* η¹:η¹:μ₂ ligation mode. Two η² chelating nitrate groups, one each on Ce4 and Ce5, complete the ligation. All Mn^{III} atoms are six-coordinate with distorted octahedral geometries, whereas Ce1 is ten-coordinate, Ce2 and Ce3 are nine-coordinate, and Ce4 and Ce5 are eight-coordinate. As expected, the Mn^{III} atoms all show a Jahn–Teller axial elongation. Complex **1** possesses C₁ crystallographic symmetry but virtual C₂ symmetry, the C₂ axis passing through Mn1, Ce1, and O3, and it is the largest discrete molecular Ce–Mn cluster reported to date.

The structure and a stereoview of [Ce^{IV}Mn^{III}₇O₈(O₂CPh)₁₇(H₂O)₄] (**2**) are shown in Fig. 2. Selected interatomic distances and bond angles are available in Table S2. Its [Ce₃Mn₇O₈]¹⁷⁺ core comprises three Ce^{IV} and seven Mn^{III} atoms held together by two μ₄-O²⁻ and six μ₃-O²⁻ ions. The metal oxidation states and protonation levels of the O atoms were again determined by inspection of metric parameters, charge considerations, and bond valence sum (BVS) calculations (Tables 2 and 3). As for the anion of **1**, the core of **2** possesses a somewhat irregular structure consisting of edge-fused triangular M₃ units, and shows some similarity as a sub-fragment of the core of **1**. There is a central Ce₃ subunit enclosed between seven Mn^{III} atoms, but unlike **1** the latter are all connected and the core can thus also be described as a serpentine (S-shaped) chain of Mn^{III} atoms around a V-shaped Ce₃ unit, all held together by the bridging O²⁻ ions. Peripheral ligation is provided by three μ₃-, twelve μ₂-, two η² chelating benzoate groups, and four terminal

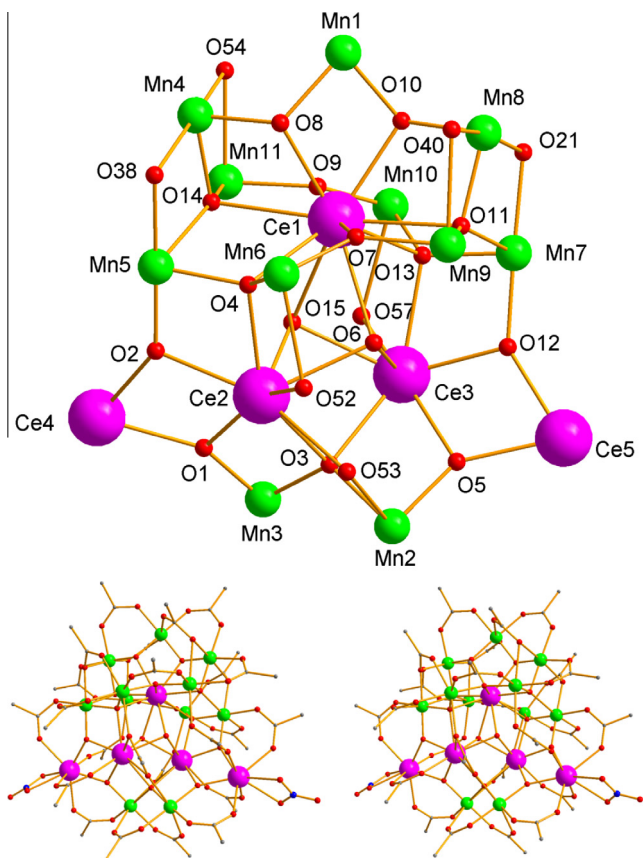


Fig. 1. (top) The labeled core of complex **1** with all ligands removed except for some doubly-bridging carboxylate O atoms, and (bottom) a stereopair of the complete structure but with Ph rings removed except for their *ipso* C atoms. Color code: Mn^{III} green, Ce^{IV} purple, N blue, O red, C gray. (Color online).

Table 2
Bond valence sums and assignments for Mn and Ce atoms in **1** and **2**.

	Atom ^a	Mn ^{II}	Mn ^{III}	Mn ^{IV}	Atom ^a	Ce ^{III}	Ce ^{IV}
1	Mn1	3.35	<u>3.07</u>	3.22	Ce1	4.28	<u>3.85</u>
	Mn2	3.32	<u>3.03</u>	3.18	Ce2	4.6	<u>4.14</u>
	Mn3	3.33	<u>3.04</u>	3.19	Ce3	4.67	<u>4.20</u>
	Mn4	3.29	<u>3.01</u>	3.16	Ce4	4.72	<u>4.25</u>
	Mn5	3.24	<u>2.96</u>	3.1	Ce5	4.68	<u>4.22</u>
	Mn6	3.3	<u>3.02</u>	3.17			
	Mn7	3.2	<u>2.93</u>	3.07			
	Mn8	3.25	<u>2.97</u>	3.12			
	Mn9	3.25	<u>2.97</u>	3.12			
	Mn10	3.27	<u>2.99</u>	3.14			
	Mn11	3.24	<u>2.97</u>	3.11			
2	Mn1	3.19	<u>2.92</u>	3.07	Ce1	4.34	<u>3.90</u>
	Mn2	3.31	<u>3.03</u>	3.18	Ce2	4.53	<u>4.07</u>
	Mn3	3.25	<u>2.98</u>	3.12	Ce3	4.73	<u>4.26</u>
	Mn4	3.25	<u>2.97</u>	3.12			
	Mn5	3.26	<u>2.98</u>	3.12			
	Mn6	3.27	<u>2.99</u>	3.14			
	Mn7	3.23	<u>2.95</u>	3.1			

^a The underlined value is the one closest to the charge for which it was calculated. The oxidation state can be taken as the nearest whole number to the underlined value.

H₂O molecules (two each on Mn1 and Mn4). The benzoates again bridge in a variety of modes: one $\eta^2:\eta^2:\mu_3$ (as in **1**) on the Ce₃ unit, two unusual $\eta^2:\eta^1:\mu_2$ on CeMn pairs, and twelve common *syn*, *syn*

Table 3
Bond valence sums and assignments for selected O atoms^a in **1** and **2**.

	Atom ^a	BVS	Assignment
1	O1	2.12	O ²⁻
	O2	2.16	O ²⁻
	O3	2.16	O ²⁻
	O4	2.1	O ²⁻
	O5	2.11	O ²⁻
	O6	1.23	OH ⁻
	O7	2.08	O ²⁻
	O8	2.08	O ²⁻
	O9	2.09	O ²⁻
	O10	2.15	O ²⁻
	O11	1.88	O ²⁻
	O12	2.16	O ²⁻
	O13	2.14	O ²⁻
	O14	1.9	O ²⁻
	O15	1.23	OH ⁻
2	O1	2.11	O ²⁻
	O2	2.11	O ²⁻
	O3	2.14	O ²⁻
	O4	2.08	O ²⁻
	O5	2.03	O ²⁻
	O6	2.19	O ²⁻
	O7	2.1	O ²⁻
	O8	2.2	O ²⁻
	O43	0.24	H ₂ O
	O44	0.27	H ₂ O
	O45	0.25	H ₂ O
	O46	0.24	H ₂ O

^a An O BVS in the ~ 1.8 – 2.0 , ~ 1.0 – 1.2 and ~ 0.2 – 0.4 ranges is indicative of non-, single- and double-protonation, respectively.

$\eta^1:\eta^1:\mu_2$. All Mn^{III} atoms are six-coordinate with near-octahedral geometries and JT elongation axes involving the O atoms of benzoate and H₂O groups, the central Ce1 is ten-coordinate, and Ce2 and Ce3 are nine-coordinate. As for **1**, the structure of **2** is unprecedented. Also as for **1**, complex **2** possesses C₁ crystallographic symmetry but virtual C₂ symmetry, the C₂ axis passing through Mn5 and Ce1.

3.3. Magnetochemistry

3.3.1. Direct current (dc) magnetic susceptibility studies

Solid-state, variable-temperature dc magnetic susceptibility measurements were performed on powdered microcrystalline samples of dried 1.5MeNO₂ and 2.2MeNO₂ in the 5–300 K range and in a 1 kG (0.1 T) field. The samples were restrained in eicosane to prevent torquing.

For 1.5MeNO₂, $\chi_M T$ decreases smoothly from 24.33 cm³ K mol⁻¹ at 300 K to a near-plateau of 17.17 cm³ K mol⁻¹ at 25 K before decreasing more steeply to 13.90 cm³ K mol⁻¹ at 5 K (Fig. 3). All the paramagnetism in the system is from Mn^{III} since Ce^{IV} is diamagnetic (f^0), and the value of 24.33 cm³ K mol⁻¹ at 300 K is much lower than the spin-only ($g = 2.0$) value expected for eleven non-interacting Mn^{III} ions of 33.00 cm³ K mol⁻¹, indicating dominant but weak antiferromagnetic (AF) interactions within the molecule. The structural separation of the eleven Mn^{III} atoms into groups of nine and two by the Ce₅ unit (Fig. 1) suggests a possible rationalization of the overall $\chi_M T$ versus T profile of Fig. 3. The higher T data could be reflecting weak AF interactions within each of the Mn₉ and Mn₂ units, and only below 25 K is an additional decrease due to antiferromagnetic exchange interactions between the two units observed; the latter are expected to be much weaker since they are through the Ce atoms. On this basis, the $\chi_M T$ at 5.0 K of 13.90 cm³ K mol⁻¹ would be consistent with a ground state of $S = 5$ (spin-only value 15.00 cm³ K mol⁻¹) for the complete molecule. Although we do not observe significant intermolecular π – π stacking in the structure, we cannot rule out weak intermolecular

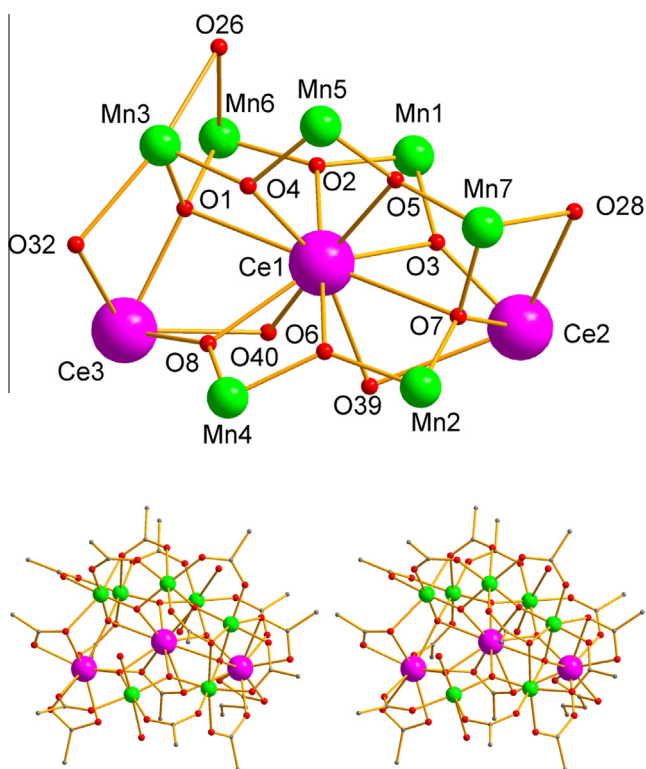


Fig. 2. (top) The labeled core of complex **2** with all ligands removed for clarity, and (bottom) a stereopair of the complete structure with Ph rings removed except for their *ipso* C atoms. Color code: Mn^{III} green, Ce^{IV} purple, N blue, O red, C gray. (Color online).

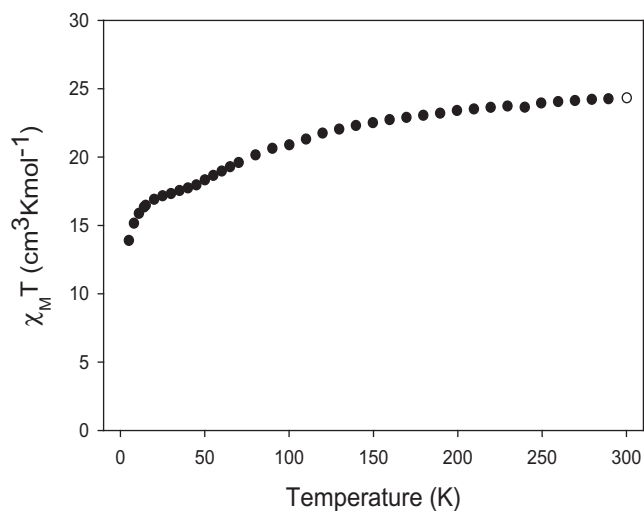


Fig. 3. Plot of $\chi_M T$ vs. T for complex **1-5MeNO**₂.

AF interactions also contributing to the decrease at the lowest temperatures.

In order to probe the ground state further, we collected magnetization (M) data in the 1.8–10 K range in applied dc fields (H) up to 7 T. Attempts were made to fit the data, using the program MAGNET [20], to a model that assumes only the ground state is populated at these temperatures and fields, and incorporates an isotropic Zeeman interaction, axial zero-field splitting ($D\hat{S}_z^2$) and a full powder average. A satisfactory fit could not be obtained, consistent with the high Mn nuclearity, and the weak AF interactions and

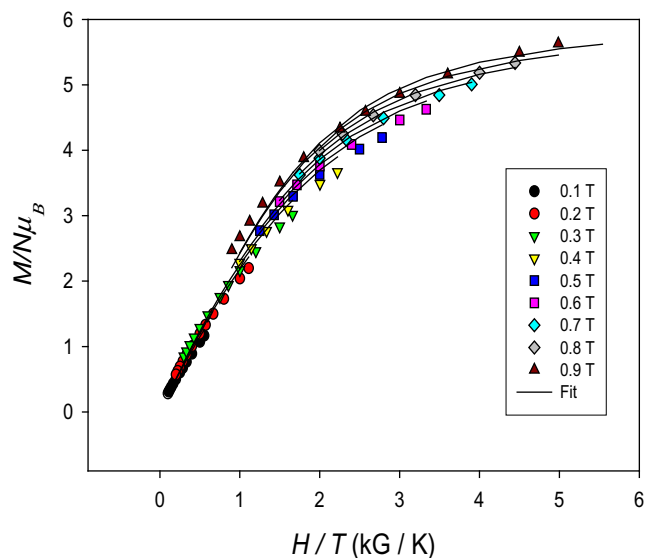


Fig. 4. Plot of $M/N\mu_B$ vs. H/T for **1-5MeNO**₂ at the indicated applied fields. The solid lines are the fit of the data; see the text for the fit parameters.

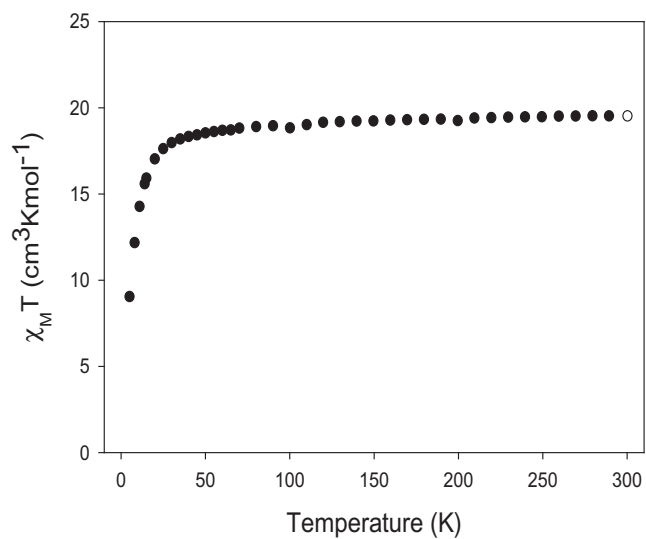


Fig. 5. Plot of $\chi_M T$ vs. T for complex **2-2MeNO**₂.

low-lying excited states expected to be present. We thus used only data collected at low fields in the 1–9 kG range to try to minimize the effect of these problems, and they are plotted in Fig. 4 as reduced magnetization ($M/N\mu_B$) versus H/T , where N is Avogadro's number and μ_B is the Bohr magneton. A fair fit was obtained with $S = 5$, $g = 1.95(4)$, and $D = -0.57(1)$ K (solid lines in Fig. 4), supporting the conclusion from the $\chi_M T$ versus T plot.

For **2-2MeNO**₂, $\chi_M T$ decreases gently from 19.52 cm³ K mol⁻¹ at 300 K to 18.19 cm³ K mol⁻¹ at 35 K, and then decreases more steeply to 9.08 cm³ K mol⁻¹ at 5 K (Fig. 5). The overall profile indicates only weak AF interactions, weaker on average than those in **1**, and indeed the value of 19.52 cm³ K mol⁻¹ at 300 K is only slightly lower than that expected for seven non-interacting Mn^{III} ions (spin-only 21.00 cm³ K mol⁻¹). Also as expected, we could obtain no reasonable fit of reduced magnetization data collected as for **1**, which is clearly due to the presence of particularly low-lying excited states.

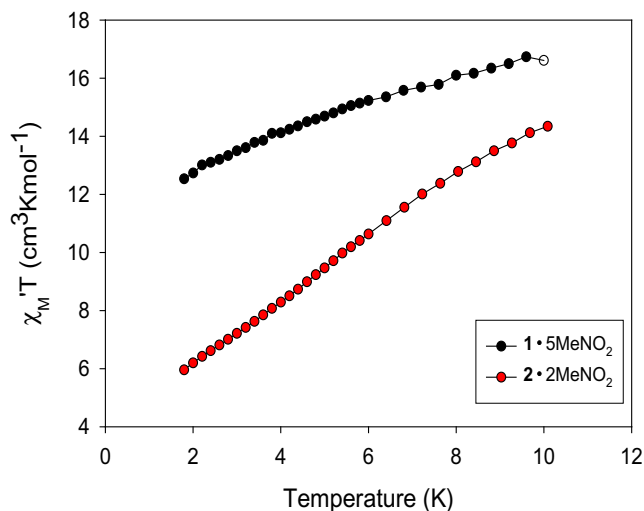


Fig. 6. Plots of ac in-phase $\chi'_M T$ vs. T for complexes **1**·5MeNO₂ and **2**·2MeNO₂ in a 3.5 G ac field at 1000 Hz oscillation frequency.

3.3.2. Alternating current (ac) magnetic susceptibility studies

As an independent probe of the ground states of **1** and **2**, ac susceptibility data were collected in the 1.8–15 K range using a 3.5 G ac field with an oscillation frequency of 1000 Hz. The ac in-phase susceptibility (χ'_M) is plotted as $\chi'_M T$ versus T for **1**·5MeNO₂ and **2**·2MeNO₂ in Fig. 6. No out-of-phase χ''_M signals were observed down to 1.8 K for either compound. For **1**·5MeNO₂, the data are in good agreement with the dc data; $\chi'_M T$ decreases with decreasing T as expected for depopulation of low-lying excited states with S greater than the ground state, as expected for weak AF interactions. The plot extrapolates to ~ 12 cm³ K mol⁻¹ supporting the conclusions from the dc data of an $S = 5$ ground state and assuming only very weak intermolecular interactions; $S = 4$ and 6 ground states would give values slightly below the spin-only 10 and 21 cm³ K mol⁻¹, respectively.

For **2**·2MeNO₂, $\chi'_M T$ decreases with decreasing T much more rapidly than for **1**·5MeNO₂, indicating particularly low-lying excited states with S greater than the ground state, supporting the conclusions from the dc data, which suggest very weak AF interactions and thus very low-lying excited states. The plot appears to be heading for ~ 4 cm³ K mol⁻¹ at 0 K, indicating a very low ground state, but it is too unreliable to be more precise for such a system. For example, a value of 4 cm³ K mol⁻¹ would be consistent with a near degenerate $S = 2/S = 3$ situation (spin-only 4.30 cm³ K mol⁻¹ for exact degeneracy), as well as other such possibilities.

4. Summary and conclusions

Two new Ce/Mn clusters with unprecedented structures and metal topologies have been synthesized and characterized. They were obtained from applying some simple modifications to the usual synthetic procedures in this area. The two compounds are somewhat structurally related to each other, and bear structural features found in other Mn and Ce clusters (e.g. M₃ triangles and M₄ butterfly units), but they nevertheless represent previously unobserved topological assemblies. Both complexes were characterized through magnetic susceptibility measurements as being predominantly weakly antiferromagnetically coupled, and seem to both possess non-zero ground states, $S = 5$ for **1** and $S = 2$ or 3 probably for **2**. The present results thus provide two new and aesthetically-pleasing members of the growing family of

Ce–Mn clusters, and 3d–4f clusters in general. Further work in Ce–Mn chemistry is in progress and will be reported in due course.

Acknowledgment

We thank the National Science Foundation for support of this work (DMR-1213030).

Appendix A. Supplementary data

CCDC 775362 and 775363 contain the supplementary crystallographic data for **1**·7MeNO₂ and **2**·6MeNO₂, respectively. These data can be obtained free of charge via <http://www.ccdc.cam.ac.uk/conts/retrieving.html>, or from the Cambridge Crystallographic Data Centre, 12 Union Road, Cambridge CB2 1EZ, UK; fax: (+44) 1223-336-033; or e-mail: deposit@ccdc.cam.ac.uk. Supplementary data associated with this article can be found, in the online version, at <http://dx.doi.org/10.1016/j.poly.2015.03.017>.

References

- [1] (a) Photosynthetic Water Oxidation, J. Nugent (Ed.), *Biochim. Biophys. Acta* (2001) 1503, 1.; (b) V.K. Yachandra, K. Sauer, M.P. Klein, *Chem. Rev.* 96 (1996) 2927; (c) R. Manchanda, G.W. Brudvig, R.H. Crabtree, *Coord. Chem. Rev.* 144 (1995) 1.
- [2] (a) W. Ruttiger, C.G. Dismukes, *Chem. Rev.* 97 (1997) 1; (b) M. Yagi, M. Kaneko, *Chem. Rev.* 101 (2001) 21; (c) J. Barber, J.W. Murray, *Coord. Chem. Rev.* 252 (2008) 233; (d) C.S. Mullins, V.L. Pecoraro, *Coord. Chem. Rev.* 252 (2008) 416.
- [3] (a) D. Arndt, *Manganese Compounds as Oxidizing in Organic Chemistry*, Open Court Publishing Company, Illinois, USA, 1981; (b) T.-L. Ho, in: W.J. Mids, C.R.H.I. de Jonge (Eds.), *Organic Syntheses by Oxidation with Metal Compounds*, Plenum, New York, 1986, pp. 569 (chapter 11); (c) B.B. Snider, *Chem. Rev.* 96 (1996) 339; (d) A. Trovarelli, *Catal. Rev.* 38 (1996) 439.
- [4] (a) Y.I. Matatov-Meytal, M. Scheintuch, *Ind. Eng. Chem. Res.* 37 (1998) 309; (b) H. Cao, S.L. Suib, *J. Am. Chem. Soc.* 116 (1994) 5334; (c) A.J. Tasiopoulos, K.A. Abboud, G. Christou, *Chem. Commun.* (2003) 580; (d) K.R. Reddy, M.V. Rajasekharan, S. Padhye, F. Dahan, J.-P. Tuchagues, *Inorg. Chem.* 33 (1994) 428; (e) K. Dimitrou, A.D. Brown, T.E. Concolino, A.L. Rheingold, G. Christou, *Chem. Commun.* (2001) 1284.
- [5] (a) S. Imamura, A. Doi, S. Ishida, *Ind. Eng. Chem. Prod. Res. Dev.* 24 (1985) 75; (b) S. Hamoudi, K. Belkacemi, A. Sayari, F. Larchi, *Chem. Eng. Sci.* 56 (2001) 1275; (c) S. Hamoudi, K. Belkacemi, F. Larachi, *Chem. Eng. Sci.* 54 (1999) 3569; (d) Z.Y. Ding, M.A. Frisch, L. Li, E.F. Gloyne, *Ind. Eng. Chem. Res.* 35 (1996) 3257.
- [6] (a) T. Lis, *Acta Cryst. B* B36 (1980) 2042; (b) S. Bhaduri, A.J. Tasiopoulos, M.A. Bolcar, K.A. Abboud, W.E. Streib, G. Christou, *Inorg. Chem.* 42 (2003) 1483; (c) K.R. Reddy, M.V. Rajasekharan, N. Arulsamy, D.J. Hodgson, *Inorg. Chem.* 35 (1996) 2283; (d) V. Nair, J. Mathew, J. Prabhakaran, *Chem. Soc. Rev.* 26 (1997) 127.
- [7] (a) G. Christou, D. Gatteschi, D.N. Hendrickson, R. Sessoli, *MRS Bull.* 25 (2000) 66; (b) G. Aromi, E.K. Brechin, *Struct. Bonding (Berlin)* 122 (2006) 1; (c) G. Christou, *Polyhedron* 24 (2005) 2065.
- [8] (a) R. Sessoli, H.L. Tsai, A.R. Schake, S. Wang, J.B. Vincent, K. Folting, D. Gatteschi, G. Christou, D.N. Hendrickson, *J. Am. Chem. Soc.* 115 (1993) 1804; (b) R. Sessoli, D. Gatteschi, A. Caneschi, M.A. Novak, *Nature* 365 (1993) 141.
- [9] R. Bagai, G. Christou, *Chem. Soc. Rev.* 38 (2009) 1011.
- [10] J.R. Friedman, M.P. Sarachik, J. Tejada, R. Ziolo, *Phys. Rev. Lett.* 76 (1996) 3830.
- [11] (a) W. Wernsdorfer, R. Sessoli, *Science* 284 (1999) 133; (b) W. Wernsdorfer, M. Soler, G. Christou, D.N. Hendrickson, *J. Appl. Phys.* 91 (2002) 7164; (c) W. Wernsdorfer, N.E. Chakov, G. Christou, *Phys. Rev. Lett.* 95 (037203) (2005) 1.
- [12] (a) C. Papatriantafyllopoulou, K.A. Abboud, G. Christou, *Inorg. Chem.* 50 (2011) 8959; (b) M. Hołynska, D. Premuzic, I.-R. Jeon, W. Wernsdorfer, R. Clérac, S. Dehnen, *Chem. Eur. J.* 17 (2011) 9605; (c) C. Papatriantafyllopoulou, W. Wernsdorfer, K.A. Abboud, G. Christou, *Inorg. Chem.* 50 (2011) 421; (d) A. Saha, M. Thompson, K.A. Abboud, W. Wernsdorfer, G. Christou, *Inorg. Chem.* 50 (2011) 10476.

- [13] (a) T.K. Prasad, M.V. Rajasekharan, J.P. Costes, *Angew. Chem. Int. Ed.* 46 (2007) 2851;
(b) C.M. Zaleski, J.W. Kampf, T. Mallah, M.L. Kirk, V.L. Pecoraro, *Inorg. Chem.* 46 (2007) 1954;
(c) G. Karotsis, S. Kennedy, S.J. Teat, C.M. Beavers, D.A. Fowler, J.J. Morales, M. Evangelisti, S.J. Dalgarno, E.K. Brechin, *J. Am. Chem. Soc.* 132 (2009) 12983.
- [14] (a) F.C. Liu, Y.F. Zeng, J. Jiao, J.R. Li, X.H. Bu, J. Ribas, S.R. Batten, *Inorg. Chem.* 45 (2006) 6129;
(b) V. Mereacre, A.M. Ako, R. Clerac, W. Wernsdorfer, G. Filoti, J. Bartolome, C.E. Anson, A.K. Powell, *J. Am. Chem. Soc.* 129 (2007) 9248;
(c) V. Mereacre, A.M. Ako, R. Clerac, W. Wernsdorfer, I.J. Hewitt, C.E. Anson, A.K. Powell, *Chem. Eur. J.* 14 (2008) 3577;
(d) S. Langley, B. Moubaraki, K.S. Murray, *Dalton Trans.* 39 (2010) 5066.
- [15] (a) H. Oshio, M. Nihei, S. Koizumi, T. Shiga, H. Nojiri, M. Nakano, N. Shirakawa, M. Akatsu, *J. Am. Chem. Soc.* 127 (2005) 4568;
(b) G.A. Timco, A.S. Batsanov, F.K. Larsen, C.A. Muryn, J. Overgaard, S.J. Teat, R.E.P. Winpenny, *Chem. Commun.* 41 (2005) 3649;
(c) W. Wernsdorfer, D. Maily, G.A. Timco, R.E.P. Winpenny, *Phys. Rev. B* 72 (060409) (2005) 1–4;
(d) W.G. Wang, A.J. Zhou, W.X. Zhang, M.L. Tong, X.M. Chen, M. Nakano, C.C. Beedle, D.N. Hendrickson, *J. Am. Chem. Soc.* 129 (2007) 1014.
- [16] O. Kahn, *Molecular Magnetism*, VCH, New York, 1993.
- [17] (a) A.J. Tasiopolous, A. Mishra, G. Christou, *Polyhedron* 26 (2007) 2183;
(b) G.V. Romanenko, E. Fursova, V.I. Ovcharenko, *Russ. Chem. Bull. Int. Ed.* 58 (2009) 1.
- [18] J.B. Vincent, K. Folting, J.C. Huffman, G. Christou, *Inorg. Chem.* 25 (1986) 996.
- [19] S.B. Yu, S.J. Lippard, L. Shweky, A. Bino, *Inorg. Chem.* 31 (1992) 3502.
- [20] E.R. Davidson, *MAGNET*, Indiana University, Bloomington, IN, 1999.
- [21] R.C. Weast, *CRC Handbook of Chemistry and Physics*, CRC Press Inc., Boca Raton, FL, 1984.
- [22] SHELXTL6; Bruker AXS: Madison, WI, 2000.
- [23] P. Vandersluis, A.L. Spek, *Acta Crystallogr. A* 46 (1990) 194.
- [24] (a) A.J. Tasiopoulos, T.A. O'Brien, K.A. Abboud, G. Christou, *Angew. Chem. Int. Ed.* 43 (2004) 345;
(b) A.J. Tasiopoulos, P.L. Milligan Jr., K.A. Abboud, T.A. O'Brien, G. Christou, *Inorg. Chem.* 46 (2007) 9678.
- [25] A. Mishra, A.J. Tasiopoulos, W. Wernsdorfer, E.E. Moushi, B. Moulton, M.J. Zaworotko, K.A. Abboud, G. Christou, *Inorg. Chem.* 47 (2008) 4832.
- [26] (a) A.J. Tasiopoulos, W. Wernsdorfer, B. Moulton, M.J. Zaworotko, G. Christou, *J. Am. Chem. Soc.* 125 (2003) 15274;
(b) A. Mishra, A.J. Tasiopoulos, W. Wernsdorfer, K.A. Abboud, G. Christou, *Inorg. Chem.* 46 (2007) 3105.
- [27] V. Mereacre, A.M. Atko, M.N. Akhtar, A. Lindermann, C.E. Anson, A.K. Powell, *Helv. Chim. Acta* 92 (2009) 2507.
- [28] C.J. Milios, P.A. Wood, S. Parsons, D. Foguet-Albiol, C. Lampropoulos, G. Christou, S.P. Perlepes, E.K. Brechin, *Inorg. Chim. Acta* 360 (2007) 3932.
- [29] C. Lampropoulos, A.E. Thuijs, K.J. Mitchell, K.A. Abboud, G. Christou, *Inorg. Chem.* 53 (2014) 6805.
- [30] G. Maayan, G. Christou, *Inorg. Chem.* 50 (2011) 7015.